

# pH-responsive hybrid nanoparticle with enhanced dissociation characteristic for siRNA delivery

Menghao Shi<sup>1</sup>  
Xiufeng Zhao<sup>2</sup>  
Jiulong Zhang<sup>1</sup>  
Shuang Pan<sup>1</sup>  
Chunrong Yang<sup>3</sup>  
Ying Wei<sup>1</sup>  
Haiyang Hu<sup>1</sup>  
Mingxi Qiao<sup>1</sup>  
Dawei Chen<sup>1</sup>  
Xiuli Zhao<sup>1</sup>

<sup>1</sup>Department of pharmaceutics, School of Pharmacy, Shenyang Pharmaceutical University, Shenyang 110016, PR China; <sup>2</sup>Oncology Department, Affiliated Hongqi Hospital of Mudanjiang Medical College, Mudanjiang 157000, PR China; <sup>3</sup>Department of pharmaceutics, School of Pharmacy, Jiamusi University, Jiamusi, Heilongjiang 154007, PR China

Correspondence: Xiuli Zhao  
Department of pharmaceutics, School of Pharmacy, Shenyang Pharmaceutical University, 103 Wenhua Road, Shenyang 110016, PR China  
Tel +86 24 2398 6306  
Fax +86 24 2398 6306  
Email raura3687yd@163.com

**Introduction:** Specific polo-like kinase (PLK1) silencing with small interface RNA (siRNA) may be an effective approach for PLK1-overexpressed lung cancer. However, low siRNA concentration into cytoplasm of tumor tissue severely limits its application.

**Materials and methods:** In this study, a novel triblock copolymer methoxy poly(ethylene glycol)-poly(histidine)-poly(sulfadimethoxine) (mPEG-PHis-PSD, shorten as PHD) was synthesized and used to construct novel nonviral gene vector with cationic liposomes.

**Results:** The resulting hybrid nanoparticles (PHD/LR) loaded with siPLK1 possessed excellent physiochemical properties. In vitro study indicated that PHD/LR could be efficiently internalized into human lung adenocarcinoma A549 cells and downregulated PLK1 protein expression to induce cell apoptosis, which was attributed to pH-induced instantaneous dissociation, efficient endo/lysosomal escape arose from PHD copolymer. Furthermore, in vivo antitumor activity demonstrated that PHD/LR could efficiently accumulated into tumor tissue and silenced PLK1 expression to possess antitumor activity.

**Conclusion:** Taken all these together, PHD/LR was expected to be a suitable carrier for specific delivering siRNA for lung cancer therapy.

**Keywords:** pH-responsive, siRNA delivery, hybrid nanoparticles, systematic evaluation

## Introduction

Lung cancer is the leading cause of death worldwide, 80% of which is due to non-small-cell lung cancer (NSCLC).<sup>1-3</sup> Most of the NSCLC patients are frequently diagnosed with advanced-stage disease and have a 5-year survival rate of only 17.4%, lower than that of many other cancer sites.<sup>4,5</sup> Despite several approaches being applied in clinical setting like radiotherapy and surgery, chemotherapy still plays an important role in the treatment of NSCLC. However, severe side effects and systematic toxicity limit its application.<sup>6-8</sup> Due to low cytotoxicity and low immunogenicity, gene therapy is becoming a powerful strategy for cancer treatment compared with conventional chemotherapy.<sup>6,9</sup> RNA interference (RNAi), triggered by siRNA, is a viable alternative to regulate specific protein expression for treatment of malignancy. Despite many advantages for RNAi technology, many barriers still exist that need to be solved. Firstly, siRNA suffers from poor cellular uptake and rapid clearance rate, which may result in low knocking-down efficacy.<sup>10,11</sup> Due to the presence of ribonuclease (RNase) in the circulatory system, siRNA will be degraded quickly after intravenous administration. Therefore, it is necessary to design an efficient carrier to deliver therapeutical agents to target site.

As a conventional nonviral vector, cationic liposomes have been proved to have efficient transfection efficacy. Unlike any chemotherapeutical agent, which involves incorporating the drug into the inner core of the carrier (or mixed with carrier), most gene vectors would load gene via simple electrostatic interactions. While it possesses

favorable *in vitro* transfection efficacy, *in vivo* activity is not up to a satisfactory level. This phenomenon can be attributed to two aspects: one is the presence of positive surface charge that would increase the interaction between carrier and serum protein and another is lipid shell would increase the recognition of reticuloendothelial system (RES) and decrease the *in vivo* circulation time. Decoration of polyethylene glycol (PEG) on the surface of carrier can not only increase circulation time but can also shield positive charge.<sup>12,13</sup> However, the disadvantage with this procedure is that PEGylation always makes the drug delivery system (DDS) too stable to release the therapeutical agent and causes insufficient therapeutical effect, offsetting the benefit expected from PEGylation.<sup>12</sup>

In order to reach longer circulation time and on-demand drug release, many researchers designed different PEG derivatives based on the tumor microenvironment. It has been reported that the pH of tumor tissue is different from that of normal tissue.<sup>13–15</sup> In particular, intracellular endo/lysosomal pH was found to be 5.0–5.5, while that of the extracellular matrix was 6.5–6.9.<sup>16</sup> Based on this phenomenon, PEG could link with certain groups and exhibit tumor microenvironment-responsive characteristic. For instance, few studies<sup>9,17,18</sup> designed a Schiff base bond-based PEG derivate (polyethylene glycol-Schiff base bond-cholesterol, shortened as PSC), which could be utilized to modify the surface of liposomes. Schiff base bond would be hydrolyzed in tumor microenvironment and facilitate therapeutical agent release. Similarly, Michel's group designed pH-sensitive PEG-lipid derivate via orthoester linker, which would be degraded in tumor at lower pH.<sup>19</sup> However, an interesting phenomenon should not be neglected: the leakage process of chemical bond in acidic pH is a chemical reaction and degradation rate is mainly dependant on the dissociation energy. Therefore, the pH-responsive capability of chemical bond was less than satisfactory. In comparison, being hypersensitive to pH and providing instantaneous response to environment, charge reversal-based pH-responsive copolymer provides opportunities to construct the required nanocarrier.<sup>20–22</sup> Sulfadimethoxine (SD) belonged to a subtype of sulfonamide, which possessed weak acidic characteristic due to the presence of readily ionizable hydrogen atom and resulted in pH-responsive characteristic. SD kept negative charge in neutral environment while instantaneous lost its charge in the acidic pH environment.<sup>23,24</sup> Therefore, poly(sulfadimethoxine) (PSD) is expected to be a promising pH-responsive biomaterial for the construction of DDS for cancer therapy. Similar to PSD, histidine (His) has also attracted extraordinary interest due to its biocompatibility and amphoteric nature.

Poly(histidine) (PHis) also owes pH-responsive characteristic due to protonated imidazole ring. Many PHis-based copolymer DDSs possessed pH-sensitive and sufficient endo/lysosomal escape characteristic.<sup>25–27</sup>

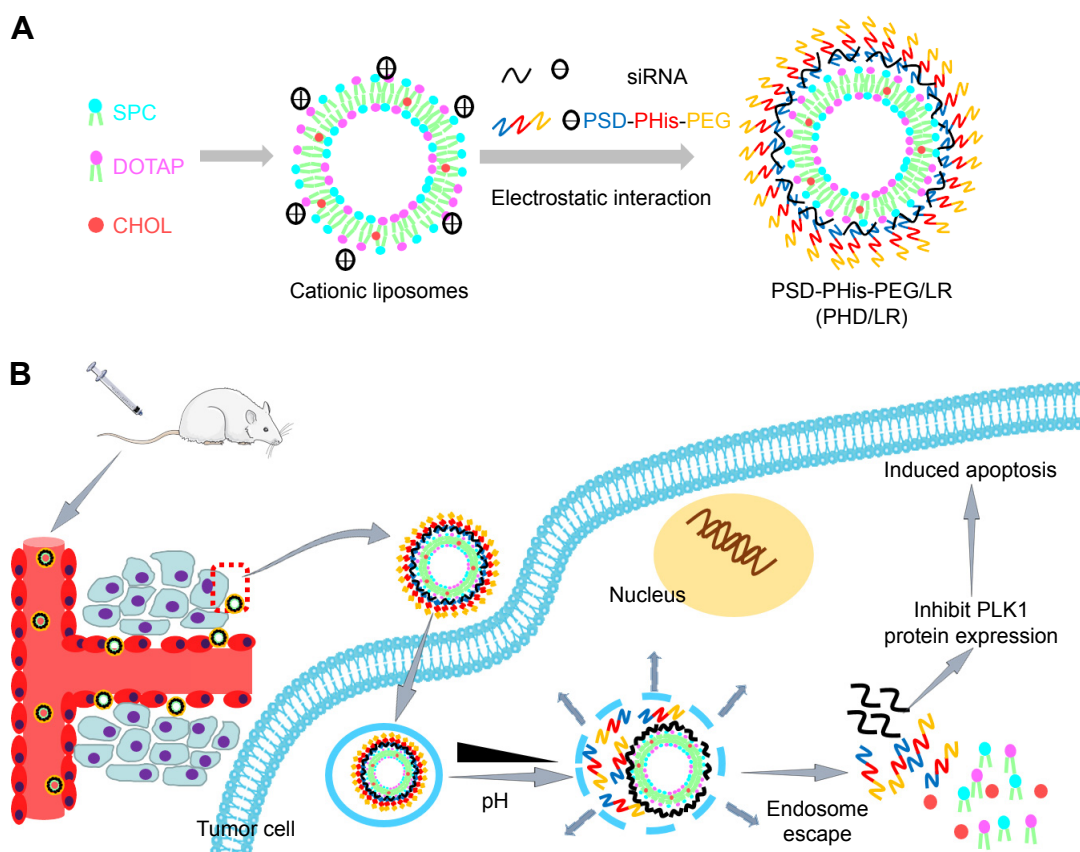
Based on the abovementioned findings, we aimed to construct a novel hybrid siRNA DDS. This DDS is composed of two parts: a cationic lipid core and a copolymer shell. Firstly, we synthesized PEG-block-PHis-block-PSD (shortened as PHD) triblock copolymer and constructed cationic liposomes. It has been reported that targeting polo-like kinase 1 (PLK1) is a promising strategy for treatment of a variety of human malignancies because it could regulate the entry into and the exit out of M-phase, spindle assembly, and dynamics as well as cytokinesis.<sup>28,29</sup> Therefore, siPLK1 was chosen as a model drug. As illustrated in Scheme 1, siRNA was interacted with cationic liposome to form lipoplex (LR) via electrostatic interaction in the first step.

The redundant positive charge could be utilized to bind PSD segment of PHD triblock copolymer to form the final hybrid nanoparticle (named PHD/LR). When PHD/LR was intravenously administered into the blood system, it would be stable due to the presence of PEG outer shell, which can not only enhance circulation time but also via electrostatic repulsion prevent the interaction between plasma proteins. PHD/LR would accumulate into tumor tissue via enhanced permeability effect (EPR) and be internalized via endocytosis process. Acidic intracellular microenvironment would transform PSD from negative charge to neutral charge, which results in a fast dissociation from LR. In endo/lysosomal pH, PHis segment would also be protonated and form proton sponge effect to accelerate intracellular siRNA delivery. Intracellular siRNA would regulate PLK1 expression and influence cell cycle, which resulted in a cell cycle arrest and apoptosis-inducing effect. Particle size,  $\zeta$ -potential, and encapsulation efficacy were all investigated and optimized. Cell cytotoxicity, cellular uptake, cell cycle, apoptosis effect, and *in vitro* PLK1 knockdown capability were all measured. *In vivo* antitumor activity was also carried out to demonstrate its therapeutical efficacy. All these results demonstrated that PHD/LR was a powerful platform to achieve tumor-selective accumulation, effective internalization, and efficient antitumor activity for safe and NSCLC therapy.

## Materials and methods

### Materials

Methoxy poly(ethylene glycol) carboxyl (mPEG-COOH, MW: 2,000 Da) was purchased from Sigma-Aldrich Co. (St Louis, MO, USA). Carboxyl-poly(histidine)-Fmoc



**Scheme 1** Schematic illustration of pH-responsive multifunctional PHD/LR (**A**) and the mechanism of accumulation into tumor tissue and exhibition of antitumor activity (**B**).

**Abbreviations:** CHOL, cholesterol; DOTAP, N-[1-(2, 3-dioleoyloxy) propyl]-N, N, N-trimethylammonium chloride; LR, lipoplex; mPEG: methoxy poly(ethylene glycol); PHD, mPEG-PHis-PSD; PHis, poly(histidine); PSD, poly(sulfadimethoxine); SPC, soybean phospholipids.

(Fmoc-NH-PHis-COOH, MW: 1,200) was synthesized from Shanghai Top-peptide Biotechnology Co., Ltd (Shanghai, China). SD, methacryloyl chloride, 2-aminoethanethiol, azodiisobutyronitrile (AIBN), 1-(3-dimethylaminopropyl)-3-ethylcarbodiimide hydrochloride (EDC), and N-hydroxylsuccinimide (NHS) were all purchased from Aladdin Biochemical Technology Co., Ltd (Shanghai, China). Soybean phospholipids (SPC), N-[1-(2, 3-dioleoyloxy) propyl]-N, N, N-trimethylammonium chloride (DOTAP), cholesterol (CHOL), and Lipofectamine 2000 were all purchased from Shanghai Advanced Vehicle Technology (AVT) Pharmaceutical Co., Ltd (Shanghai, China). MTT was purchased from Meilun Biotechnology (Dalian, China). DMEM, RPMI 1640 medium, and FBS were all supplied from Thermo Fisher Scientific (Waltham, MA, USA). Lyso-Tracker Red, Hoechst 33258, Annexin V-FITC apoptosis detection kit, and cell cycle detection kit were all purchased from Meilun Biotechnology. PLK-1,  $\beta$ -actin primary antibodies and horseradish peroxidase (HRP)-conjugated secondary antibody, and Alexa Fluor 488 and 594-conjugated secondary antibody were purchased from Proteintech Group (Rosemont,

IL, USA). SDS-PAGE gel preparation kit, enhanced chemiluminescence (ECL) kit, in situ cell death kit (TUNEL), and H&E staining kit were all purchased from Boster Biological Technology Co. Ltd (Hubei, China). All other reagents were obtained from Yuwang Co. Ltd and were of analytical grade. siPLK1 and FAM-siPLK1 were obtained from Shanghai GenePharma Co., Ltd (Shanghai, China) (sense: 5'-UGA AGA UCU GGA GGU GAA ATT-3', antisense: 5'-UUU CAC CUC CAG AUC UUC ATT-3').

## Cell culture

Human lung adenocarcinoma A549 cells and human lung epithelial cell line BEAS-2B were purchased from Chinese Academy of Sciences (Shanghai, China) and cultured in DMEM containing 10% FBS and 1% of penicillin-streptomycin solution. Cells were cultured at 37°C in a humidified atmosphere with 5% CO<sub>2</sub>.

## Animal study

Male nude mice were purchased from Shenyang Changsheng Biotechnology Co. Ltd. All the animal experiments were

performed in accordance with the Experimental Animal Administrative Committee of Shenyang Pharmaceutical University, and the study was approved by the committee. All the mice were injected with A549 cells ( $1 \times 10^7$  cells, suspended in 200  $\mu\text{L}$  PBS) into the left back to establish subcutaneous tumor according to the reference.<sup>30,31</sup> When the tumor reached  $\sim 100 \text{ mm}^3$ , they were divided randomly into several groups (control, free siRNA, LR, PD/LR, and PHD/LR,  $n=10$ ) and marked using picric acid.

## Synthesis of copolymer

### Synthesis of PSD

The synthesis route of PSD was according to the reference protocol described elsewhere<sup>23,24</sup> with minor modifications. In brief, SD and sodium hydroxide (1:1, mol/mol) were added to the round bottomed flask and dissolved with acetone/water (1:1, v/v). The mixture was cooled to  $0^\circ\text{C}$  and excess methacryloyl chloride was added into the mixture until the white precipitate could be observed. The precipitate was washed using methanol/water (10%, v/v) and vacuum dried. A white product was obtained, and was named as VSDM (vinylated SD).

VSDM, AIBN, and 2-aminoethanethiol (1:0.002:0.2, mol/mol/mol) were all dissolved in anhydrous dimethylformamide (DMF) and protected with nitrogen atmosphere. The mixture was allowed to react at  $70^\circ\text{C}$  for 48 hours. After the reaction, the mixture was poured into water and the precipitate was collected. The precipitate was washed with methanol and vacuum dried, and PSD was thus obtained. Different copolymers were characterized using  $^1\text{H-NMR}$  spectrum.

### Synthesis of PHis-PSD (PD)

Fmoc-NH-PHis-COOH, NHS, and EDC (1:2:2, mol/mol/mol) were all dissolved in anhydrous dimethyl sulfoxide (DMSO) and reacted overnight under the protection of nitrogen to activate carboxyl group of PHis. After that, the mixture was dropped into cold diethyl ether for two times and the precipitate was collected, which was Fmoc-PHis-PSD. Fmoc-PHis-PSD was then dissolved in 10 mL of anhydrous DMSO and 2 mL of diethylamine. The mixture was reacted at room temperature for 2 hours and then precipitated in cold diethyl ether. PD was finally obtained after vacuum drying.

### Synthesis of PEG-PHis-PSD (PHD)

mPEG-COOH, NHS, and EDC were dissolved in anhydrous DMSO and allowed to react for 24 hours at room temperature. Then PSD or PHis-PSD were added into the mixture and further reacted for 2 days. The mixture was dialysed against water using a dialysis bag (MWCO:3.5 kDa) for

2 days, followed by freeze drying, and PHD or PD was thus obtained.

## Preparation of different formulations

Prior to the preparation of lipoplexes, a cationic liposome was prepared first by using thin-film hydration method as reported previously.<sup>8,18</sup> In brief, SPC, DOTAP, and CHOL (4:8:2, w/w) were dissolved in chloroform/methanol (3:1, v/v). The organic solvent was removed using rotary evaporation at  $37^\circ\text{C}$  and a dry lipid film was obtained. The lipid film was rehydrated with RNase-free water at  $55^\circ\text{C}$  for 10 minutes and then sonicated (100 W for 2 minutes) with probe-type sonicator. After filtration, blank cationic liposomes (named L) were obtained.

For the preparation of siRNA-loaded LRs, L and siRNA were gently mixed and incubated at room temperature (named LR) with different N/P ratios (N and P represent amino group from DOTAP and phosphate group from siRNA, respectively).

The excess positive charge from LR was smartly utilized to interact with the negative charge of PSD from PHD copolymer to form different hybrid nanoparticles. In brief, LR and PHD (or PD) were gently mixed and incubated at room temperature with different molar ratio, which were named as PHD/LR and PD/LR, respectively.

## Characterization of different formulations

The encapsulation efficiency (EE, %) of different nanoparticles was measured by ultra-filtration method using Amicon Ultra-4 centrifugal filter devices. In brief, FAM-conjugated siRNA was used to prepare different LRs and formulations were added into the device with a centrifugal speed of 4,000 rpm for 10 minutes. Free siRNA was collected and measured according to a standard curve (data not shown). The EE (%) of different formulations was calculated according to the formula:

$$\text{EE \%} = \frac{C_t - C_u}{C_t} \times 100$$

where  $C_t$  and  $C_u$  represented the amount of total siRNA and unloaded siRNA, respectively.

Particle size distribution and  $\zeta$ -potential of different formulations were measured using dynamic light scattering instrument (Zetasizer Nano ZS). The morphology of hybrid nanoparticles was observed using transmission electron microscopy (TEM, HT770; Hitachi, Tokyo, Japan) and atomic force microscopy (AFM), respectively.



In order to evaluate the pH-sensitivity of PHD/LR, it was diluted with PBS at different pH (pH 7.4 and 5.0) and at different time points, and  $\zeta$ -potential of different samples were measured.

## Agarose gel electrophoresis

Agarose (with ethidium bromide in gel) was dissolved in Tris-borate-ethylenediaminetetra-acetic acid buffer to prepare 2% (w/w) agarose gel and used for electrophoresis analysis. LRs with different N/P ratios were prepared and electrophoresed in agarose gel at 100 V for 30 minutes. Naked siRNA was used as negative control. After electrophoresis, the gel was photographed and analyzed using Tanon 2500R automatic digital gel image analysis system.

For the heparin decomplexation assay, different formulations (fixed N/P ratio was 4 and copolymer: siRNA molar ratio was 3) were mixed with different heparin (heparin/siRNA, IU/ $\mu$ g) concentrations and incubated for 15 minutes at room temperature. Then different formulations were electrophoresed in agarose gel and analyzed.

For serum stability assay, different formulations were gently mixed with 50% (v/v) FBS concentration and incubated at 37°C. At different time points, samples were taken, incubated with excess heparin to replace siRNA, and electrophoresed.

## In vitro serum stability assay

In order to evaluate whether our formulations possessed favorable serum stability, in vitro stability assay was carried out in the presence of FBS. In brief, different formulations were mixed with FBS to obtain a final FBS concentration of 50% (v/v). At different time points, samples were taken and particle size distribution was measured as described earlier.

## In vitro gene release assay

In vitro siRNA release assay was investigated at different pH according to our previous report.<sup>6</sup> Briefly, different formulations were separately cultured in HEPES buffer with different pH (7.4 and 5.0) at 37°C. At scheduled time point, samples were taken out and centrifuged at 5,000 rpm for 5 minutes. Supernatants were taken and measured with ES-2 spectrophotometer (E-spect; Malcom, Tokyo, Japan).

## Cell cytotoxicity assay

Standard MTT assay was carried out to evaluate the cytotoxicity of different formulations. A549 cells and BEAS-2B cells were seeded into 96-well plate at a density of  $5 \times 10^3$  cells

per well and allowed to attach to plate surface. Blank formulations/siRNA-loaded formulations were added into each well and incubated. Twenty microliters of MTT solution ( $5 \text{ mg/mL}^{-1}$ ) was added into each well and further incubated for 4 hours. All the culture medium was removed and 100  $\mu$ L of DMSO was added. The plate was allowed to vortex and measured at 590 nm with microplate reader.

## Cellular uptake assay

Both fluorescence microscopy and flow cytometry measurement (FCM) were used to measure the cellular uptake level of different formulations. For fluorescence microscopy, cells were seeded into six-well plate with  $1 \times 10^5$  cells per well to allow attachment. The medium was replaced with serum-free RPMI 1640, and different FAM-siRNA-loaded formulations were added into each well and incubated. At scheduled time points, medium was removed and the cells were washed with PBS. The cells were fixed with formalin, stained with Hoechst 33258, and finally visualized with fluorescence microscopy.

Flow cytometry was also used to quantitatively analyze the samples. Briefly, cells were seeded into six-well plate with  $1 \times 10^6$  cells per well to allow attachment. Then the culture medium was replaced with RPMI 1640, and different FAM siRNA-loaded formulations were added into each well. The cells were collected, washed with PBS, and finally analyzed using FCM.

## Western blotting and immunofluorescence

Cells were cultured into six-well plates with  $1 \times 10^5$  cells per well to allow attachment, and different siPLK1-loaded formulations were added into each well after the replacement of DMEM with RPMI 1640 and cultured for 48 hours. Cells were collected, lysed with RIPA lysis buffer, (Beyotime Biotechnology, Shanghai, China), and the protein concentration was determined using BCA kit (Beyotime Biotechnology). The steps followed were according to the standard Western immunoblotting protocol.

Immunofluorescence assay was used to observe PLK1 expression after treatment with different formulations. In brief, cells were seeded into glass-covered six-plate wells with  $1 \times 10^5$  cells per well to allow attachment. The culture medium was replaced with RPMI 1640, and different formulations were added into each well and incubated for 48 hours. The cells were then washed with PBS and fixed with cold acetone. PLK1 protein was stained with PLK1 primary antibody and Alexa Fluor 488-conjugated secondary antibody (Proteintech Group), while  $\beta$ -actin was stained with  $\beta$ -actin primary antibody and Alexa Fluor 594-conjugated secondary

primary, respectively. The cells were finally visualized using laser scan confocal microscopy (LSCM).

### Intracellular drug release assay

In order to observe whether PHD/LR possessed endo/lysosomal escape capability, LSCM was used to observe the drug release profiles. Briefly, cells were seeded into glass-covered six-well plates and allowed to attach. Then the medium was removed by RPMI 1640 containing Lyso-Tracker Red fluorescence dye to stain endo/lysosomes for 1 hour. After that, cells were treated with FAM-siRNA-loaded PHD/LR. The cells were washed with PBS, stained the nucleic acid with Hoechst 33258, and observed using LSCM. Chloroquine was used to regulate the pH of acidic organelles prior to the study.

### Cell cycle and cell apoptosis assay

Cell cycle and cell apoptosis were both measured using FCM according to the reference protocol.<sup>30</sup> Briefly, cells were seeded into six-well plates to allow attachment. Then different formulations were added into each well and further incubated for 48 hours. The cells were then collected and further operations performed were according to the manufacturer's instructions (cell cycle detection kit and cell apoptosis detection kit; Beyotime Biotechnology).

### In vivo biodistribution assay

In vivo biodistribution assay was carried out using the nude mice from animal study "2.3". 1, 10-Dioctadecyl-3, 3, 30, 30-tetramethyl indotricarbocyanine iodide (DiR; Thermo Fisher Scientific) was used as a fluorescence probe and incorporated into different formulations. The fluorescence-labeled formulations were intravenously administered through tail vein with the same DiR concentration and allowed for distribution. After 24 hours, the mice and major organs were anesthetized and imaged using in vivo image system (Carestream Health, Rochester, NY, USA).

### In vivo antitumor activity

Male nude mice from "2.3" were used to study the in vivo antitumor activity by intravenously administering different formulations every 2 days for four times. The body weight and tumor volume were both measured. At the end of the study, mice were killed and tumor tissues were obtained, weighted, and fixed with formalin for further use.

Tumor volume was calculated using the formula:

$$V = \frac{a \times b^2}{2}$$

where  $a$  and  $b$  represent the larger diameter and the shorter diameter, respectively, of tumor tissue.

### Histological study

Tumor tissues were fixed with formalin to prepare paraffin-embedded slides (5  $\mu$ m thickness) and then stained with H&E, and TUNEL assay was performed according to the manufacturer's instructions. The excess tumor tissues from different groups were used to measure PLK1 expression at histological level (Western blotting and immunofluorescence). The detailed operation was similar with western blotting and immunofluorescence.

### Statistical analyses

Results are indicated as mean  $\pm$  SD. Two-tailed Student's  $t$ -test and one-way ANOVA were used for significant test of difference. Statistical significance was set at  $P < 0.05$  and  $P < 0.01$ .

## Results and discussion

### Synthesis of different copolymers

The synthesis pathway and <sup>1</sup>H-NMR spectrum of PHD have been illustrated in Figures S1 and S2. Vinylated SD (VSMD) was synthesized first and PSD was further synthesized using free-radical solvent polymerization method.<sup>23,24</sup> The presence of peaks at 3.72 ppm (–OCH<sub>3</sub> from SD), 5.93 ppm (–H from pyrimidine ring), and 10.09 ppm (–NH– from benzene) indicated PSD was synthesized successfully.

Fmoc-NH-PHis-COOH and PSD were synthesized via simple amidation reaction. After the reaction, Fmoc protection group was removed to expose free –NH<sub>2</sub> group to obtain PHis-PSD copolymer. The appearance of peaks at 5.98 ppm (–N= CH–C– from imidazole ring), 5.88 ppm (–CH= NH–C– from imidazole ring), and 3.81 ppm (–CH<sub>2</sub>–NH–O– from PHis) indicated that PHis-PSD was synthesized successfully.

mPEG-COOH was reacted with PHis-PSD to obtain PHD. The appearance of characteristic peaks at 2.88 ppm (–CH<sub>2</sub>–CH<sub>2</sub>–O– from PEG), 5.54 ppm (–CH= NH–C– from imidazole ring), 9.91 ppm (–NH–CO– from PSD), and 7.72 ppm (–SO<sub>2</sub>–C<sub>6</sub>H<sub>4</sub>– from PSD) indicated that triblock copolymer mPEG-PHis-PSD (PHD) was synthesized successfully.

### Characterization of different formulations

In order to prepare PHD/LR, a conventional cationic liposome was fabricated using thin film hydration method and DOTAP was utilized to provide positive charge to liposomes. As indicated in Table 1, blank liposomes (named L) possessed strong positive charge ( $\zeta$ -potential was  $\sim$ 46 mV),

**Table 1** Characterization of liposomes and LR with N/P ratio of 4 and copolymer: siRNA ratio of 3 (n=3)

Formulations	Diameter (nm)	Zeta potential (mV)	Polydispersity index	Encapsulation efficacy (%)
L	82.4±1.3	45.7±2.9	0.120±0.01	–
LR	157.2±3.4	23.8±0.3	0.118±0.01	90.2±1.4
PD/LR	179.5±2.1	4.89±0.7	0.189±0.02	91.3±1.3
PHD/LR	187.6±2.4	3.74±0.3	0.183±0.02	91.9±0.55

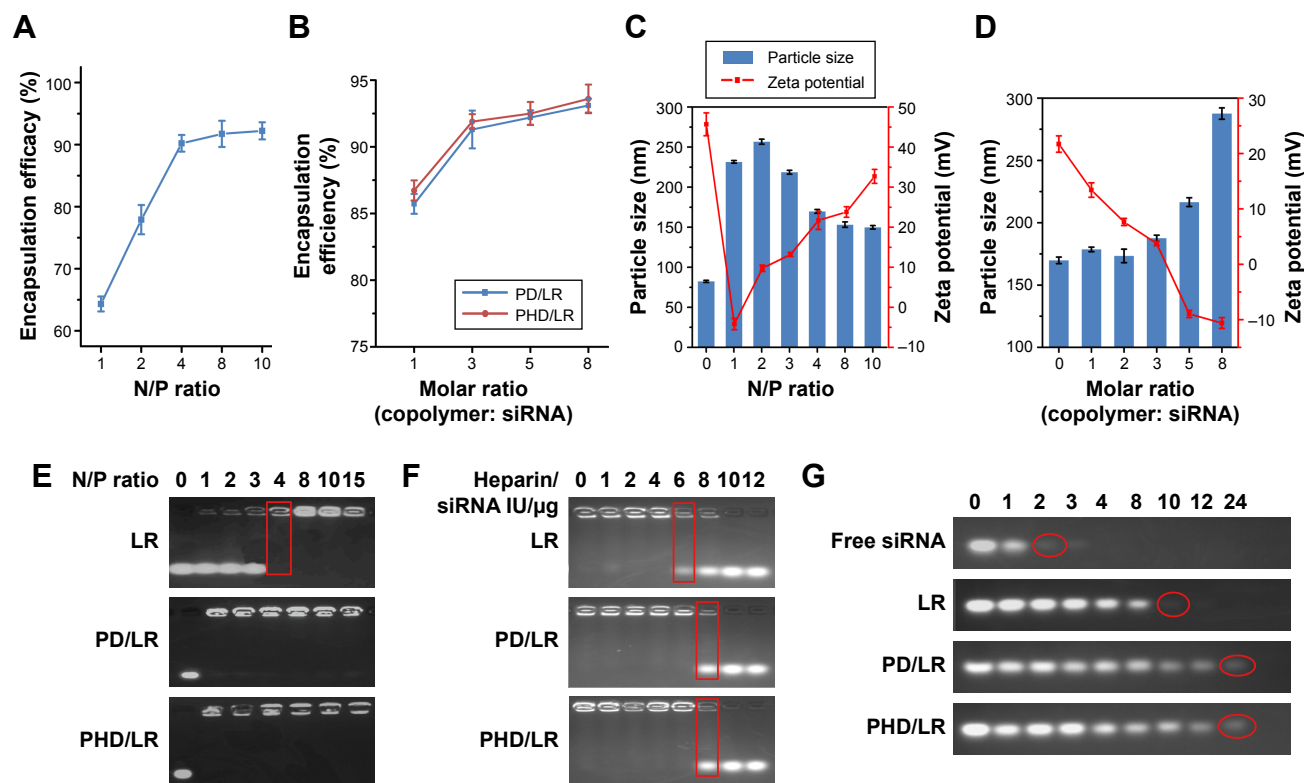
**Abbreviations:** L, liposomes; LR, lipoplex; mPEG: methoxy poly(ethylene glycol); PD, PHis-PSD; PHD, mPEG-PHis-PSD; PHis, poly(histidine); PSD, poly(sulfadimethoxine).

which indicated L exhibited favorable siRNA binding capability. Meanwhile, particle size (–80 nm) and polydispersity index (PDI, –0.12) suggested that L were uniform in size. In general, when the size of nanoparticle was above 50 nm, they showed favorable excellent retention capability when administered intravenously into the blood system.<sup>31,32</sup> Therefore, blank L were suitable carriers for further application.

In addition, siRNA and L were gently mixed and incubated at room temperature with different N/P ratios. EE (%) of different formulations was measured. As shown in Figure 1A, there was an increase of EE (%) with an increase of N/P ratio. When N/P ratio reached 4, EE (%) could reach a value above 90%. Meanwhile, particle size and  $\zeta$ -potential

of different formulations were also measured (Figure 1C); when N/P reached 4, LR possessed favorable particle size (–160 nm) and  $\zeta$ -potential (–24 mV). The excess positive charge was used to bind PSD segment from PD or PHD copolymer to prepare PD/LR or PHD/LR. Therefore, we choose 4 as the final N/P ratio for further studies.

LR was mixed with PD or PHD to prepare PD/LR or PHD/LR, and copolymer: siRNA ratio (mol/mol) was optimized as well. As shown in Figure 1B, there was an increase in EE (%) with an increase of copolymer ratio, indicating the introduction of copolymer plays a positive role in the formulation of hybrid nanoparticles. This phenomenon was probably because the electrostatic interaction between

**Figure 1** Optimization of different formulations.

**Notes:** (A) EE (%) verification with an increase of N/P ratio of L; (B) EE% verification with an increase of copolymer: siRNA ratio; (C) particle size and  $\zeta$ -potential verification with an increase of N/P ratio of L; (D) particle size and  $\zeta$ -potential verification with an increase of copolymer: siRNA ratio; (E) agarose gel electrophoresis analysis of different formulations with different N/P ratios; (F) heparin decomplexation assay of different formulations with different ratios; (G) serum stability of different formulations.

**Abbreviations:** EE, encapsulation efficiency; L, liposomes; LR, lipoplex; mPEG, methoxy poly(ethylene glycol); PD, PHis-PSD; PHD, mPEG-PHis-PSD; PHis, poly(histidine); PSD, poly(sulfadimethoxine).

copolymer and LR would compress siRNA and more siRNA would bind to the carrier. When the ratio reached a value of 3, EE (%) of PD/LR and PHD/LR were ~93%, which was higher than LR (~90%). As shown in Figure 1D, particle size and  $\zeta$ -potential were also optimized. When the ratio reached 3, particle size and  $\zeta$ -potential of PHD/LR were 187 nm and 3.74 mV, respectively, which were suitable for in vitro and in vivo studies. Therefore, copolymer: siRNA ratio was fixed at a value of 3.

## Agarose gel electrophoresis

Agarose gel electrophoresis was also used to validate whether the ratio obtained was suitable. As shown in Figure 1E, when N/P ratio reached a value of 4, all siRNAs exhibited complete retardation. Meanwhile, both PD/LR and PHD/LR showed complete retardation as well when the N/P ratio was 4 and the copolymer: siRNA ratio was 3, which was similar to the findings of our study.

Heparin decomplexation assay was carried out to investigate the stability of different formulations. As shown in Figure 1F, when the ratio reached 6, siRNA was replaced by heparin from carrier and a light strip could be observed for LR. While siRNA strip could be observed when the ratio reached 8 for both PD/LR and PHD/LR, indicating the introduction of copolymer on the surface of LRs would

increase its stability. Figure 1G illustrates the serum stability of different formulations. Naked siRNAs suffer from poor serum stability and the strip disappeared when incubation time reached 2 hours. However, LR possessed higher serum stability, and siRNA was degraded when incubated for 10 hours. Additionally, both PD/LR and PHD/LR possessed extraordinary serum stability, indicating copolymer-decorated LRs exhibited higher buffer capability against complex physiological environment.

## Morphology, pH-sensitivity, and in vitro release of different formulations

From the results obtained earlier, we finally fixed N/P ratio of 4 and copolymer: siRNA ratio of 3 as optimized prescription. The particle size,  $\zeta$ -potential, PDI, and EE (%) of different formulations have been listed in Table 1 and Figure 2A and B illustrates the morphology of PHD/LR using TEM, which exhibited spherical-shaped particles. A light outer shell (red concentric circle) could be observed from TEM, which might be PHD copolymer on the surface of the LRs. AFM image (Figure 2C) also indicated PHD/LR was a spherical shaped particle. All these data indicated the successful fabrication of PHD/LR.

In order to evaluate whether PHD or PD copolymer could dissociate from LR,  $\zeta$ -potential verification of different

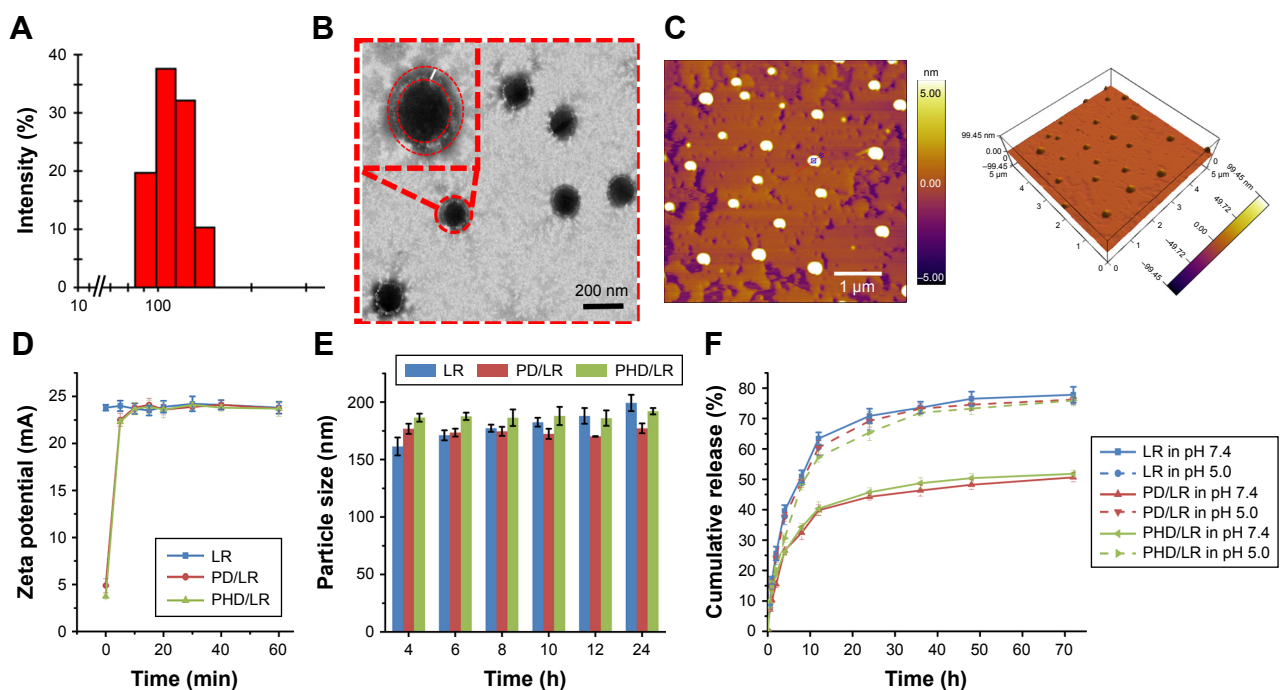


**Figure 2** Characterization of different formulations. (A) Particle size distribution of PHD/LR; (B) TEM images of PHD/LR, scale bar =200 nm; (C) AFM images of PHD/LR, scale bar =1  $\mu$ m; (D) in vitro pH sensitivity analysis; (E) in vitro serum stability assay of different formulations; (F) in vitro siRNA release of different formulations.

**Abbreviations:** AFM, atomic force microscopy; LR, lipoplex; mPEG, methoxy poly(ethylene glycol); PD, PHis-PSD; PHD, mPEG-PHis-PSD; PHis, poly(histidine); PSD, poly(sulfadimethoxine); TEM, transmission electron microscopy.



formulations were done under acidic pH. As shown in Figure 2D,  $\zeta$ -potential of LR was found to be +23.8 mV, while those of both PHD/LR and PD/LR were nearly electrically neutral. When the pH was kept as 5.0,  $\zeta$ -potential of both PHD/LR and PD/LR increased to +22.5 mV in 5 minutes, while equal to LR in the later time point. This interesting phenomenon was mainly attributed to the dissociation of PSD from LR and exposure of positive charge of LR, which indicated PHD or PD copolymer exhibited pH-responsive induced dissociation capability. This result supported favorable evidence for further *in vitro* and *in vivo* study.

*In vitro* serum stability was also investigated through observing the variation of particle size. As shown in Figure 2E, with an increase of incubation time, significant increase could be observed for LR group. It is well known that serum contains a large variety of proteins such as globulins, which would interact with positively charged nanoparticles via electrostatic interaction.<sup>16</sup> Therefore, the increase of particle size was probably because of non-specific interactions between LR and serum proteins. In comparison, both PD/LR and PHD/LR possessed satisfied serum stability due to the presence of copolymer shell, which could prevent the interaction between protein and carrier.

*In vitro* drug release experiment was performed under different pH (pH 7.4 and 5.0). As shown in Figure 2F, LR showed a burst release in the first 12 hours (63.4% at pH 7.4), followed by a sustained release at both pH values. Meanwhile, LR showed no significant difference in siRNA release behavior at both pH values, suggesting pH value did not influence LR siRNA release. In comparison, both PD/LR and PHD/LR possessed significant pH-sensitive characteristics; only about 35% of siRNA was released in neutral pH, while ~60% was released in acidic pH. This phenomenon was mainly attributed to the existence of PD or PHD. The presence of copolymer would increase binding stability of siRNA in normal pH. However, in acidic pH, the electron property of PSD changed from negative charge to neutral. This phenomenon would make PHD or PD segment dissociate instantaneously from LR and facilitate siRNA release in tumor microenvironment. It is noted that although PHis fragment also shows pH-sensitivity, imidazole ring from PHis could protonate in acidic pH, it would not influence the electron property of PHD copolymer. Therefore, there was no significant difference for both PHD/LR and PD/LR at both pH values.

From all the abovementioned results, we could realize that PHD/LR possessed good serum stability, excellent pH-sensitive characteristics, and fast siRNA release in acidic

microenvironment. These results were mainly attributed to the existence of PSD fragment, which could show charge-reversal property and facilitate siRNA release to accomplish higher therapeutical effect.

## In vitro cytotoxicity assay

A standard MTT method was used to evaluate the cytotoxicity of different siRNA-loaded and blank formulations. First, cell cytotoxicity of blank formulations was investigated. As shown in Figure 3A, with an increase of carrier concentration, no obvious cytotoxicity could be observed for PD/LR or PHD/LR, and the cell viability was above 85%, indicating both formulations were non-toxic and safe. However, LR possessed moderate toxicity at a higher concentration; this phenomenon was mainly because the cationic carrier would interact with cell membrane and cause non-specific toxicity. As shown in Figure 3B and C, cell cytotoxicity of different siRNA-loaded formulations was measured and  $IC_{50}$  values were calculated. Compared with free siRNA, LR possessed higher cytotoxicity against A549 cell line. Both copolymer decorated formulation groups showed a slightly lower cytotoxicity. This was mainly attributed to the existence of PEG shell on the surface of formulations, resulting in a weak repulsion between carrier and cell. Compared with PHD/LR group, PD/LR showed lower cytotoxicity, which indicated that the presence of PHis fragment would facilitate siRNA release into the cytoplasm and enhance therapeutical efficacy. Meanwhile, BEAS-2B cell line was also used as control to evaluate whether these formulations exhibited cytotoxicity toward normal cell. As shown in Figure 3D–F, no significant toxicity could be observed for blank formulations, indicating these formulations were non-toxic and safe for clinical applications. However, cell cytotoxicity could be observed for siRNA-loaded formulations, which showed a similar trend with A549 cell line. This phenomenon was mainly because PLK1 plays a critical role in cell cycle and the downregulation of PLK1 can arrest cell cycle, which resulted in cell cytotoxicity.

## Cellular uptake assay

Fluorescence microscopy and FCM were both used to measure the cellular uptake of different formulations; FAM-siRNA was loaded into the formulations. As shown in Figure 4A, only a weak green fluorescence could be observed for free siRNA group, indicating free siRNA suffered poor cellular uptake. LR showed the strongest green fluorescence, indicating cationic liposome is a suitable siRNA carrier for intracellular delivery of therapeutical agent. Compared with

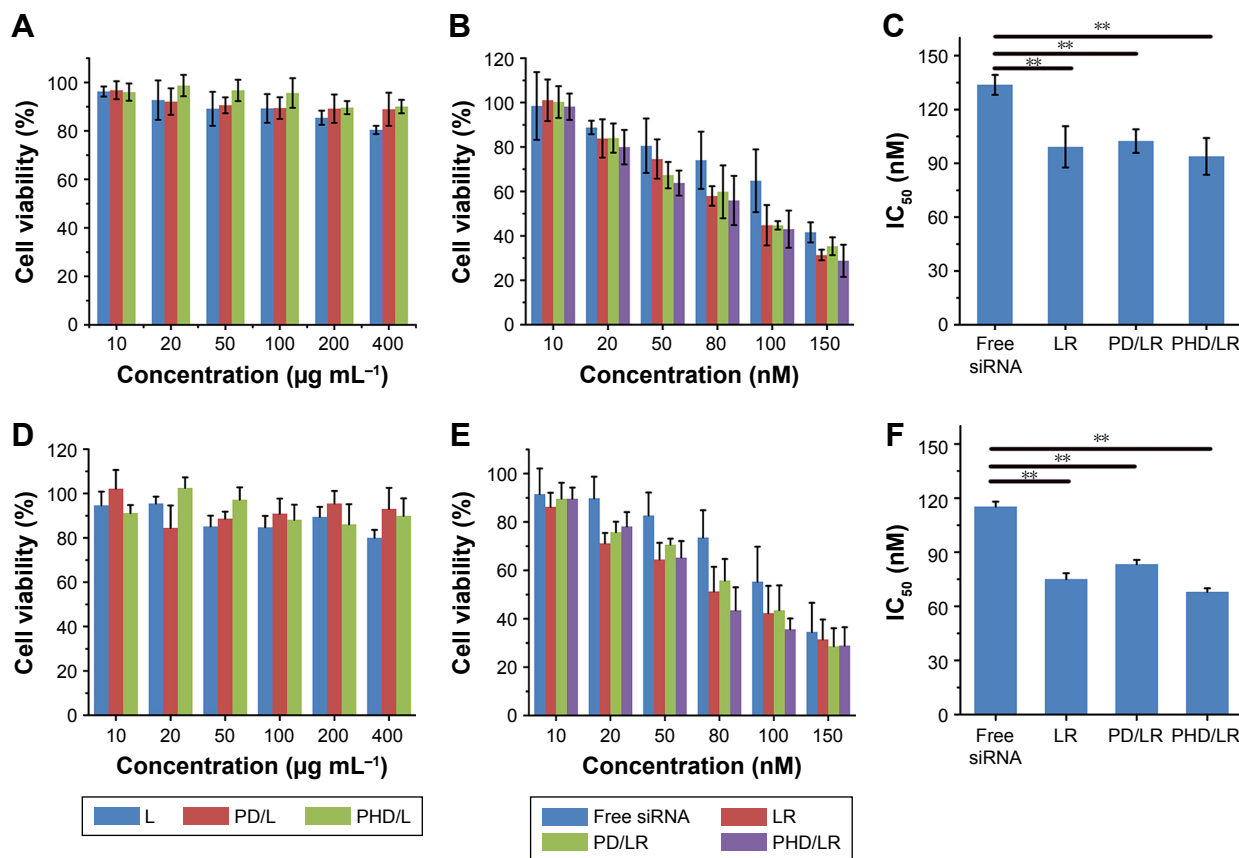


**Figure 3** In vitro cell cytotoxicity of different blank formulations (A, D) and siPLK1-loaded formulations (B, E); IC<sub>50</sub> values of different siPLK1-loaded formulations (C, F) against A549 cell line and BEAS-2B cell line, respectively.

**Note:** \*\* $p < 0.01$ .

**Abbreviations:** L, liposomes; LR, lipoplex; mPEG, methoxy poly(ethylene glycol); PD, PHis-PSD; PHD, mPEG-PHis-PSD; PSD, poly(sulfadimethoxine); PHis, poly(histidine).

PD/LR, PHD/LR possessed higher uptake behavior, and this result was in alignment with the MTT assay. As shown in Figure 4B and C, FCM was also used to quantitatively analyze the cellular uptake level of different formulations. With an increase of incubation time, green fluorescence increased gradually, indicating cellular uptake was a time-dependent property. FCM result was similar to that obtained with fluorescence microscopy, which showed that the difference in cytotoxicity was mainly attributed to different cellular uptake level.

### In vitro PLK I protein expression

The results obtained in our study indicated that siRNA could be efficiently internalized into cytoplasm and also possessed antitumor activity. Therefore, we are interested to investigate whether this cytotoxicity was attributed to the downregulation of PLK1 protein by using the technique of Western blotting (WB). As shown in Figure 5A, Lipofectamine 2000 was used as positive control. Control group possessed high PLK1 expression, while positive control group possessed

significant lower PLK1 expression. Different siRNA-treated groups possessed different degrees of PLK1 knockdown capability. LR possessed the highest knockdown capability among all groups, while PHD/LR group showed similar capability. Meanwhile, immunofluorescence (IF) was also used to observe PLK1 expression. As shown in Figure 5B, green fluorescence indicated PLK1 expression, while red fluorescence indicated  $\beta$ -actin. The intensity of green fluorescence was consistent with WB assay, proving PLK1 knockdown capability from a different perspective.

### Cell cycle and apoptosis-inducing study

It has been reported that PLK1 protein is important for numerous aspects of mitotic progression, including centrosome maturation, proper assembly of mitotic spindle, and activation of the anaphase promoting complex.<sup>29,33</sup> Meanwhile, downregulation of PLK1 would prevent cell cycle at G<sub>2</sub>/M phase and inhibit tumor growth. Therefore, we are interested to investigate the influence of different formulations on cell cycle. As shown in Figure 6A and B, control group

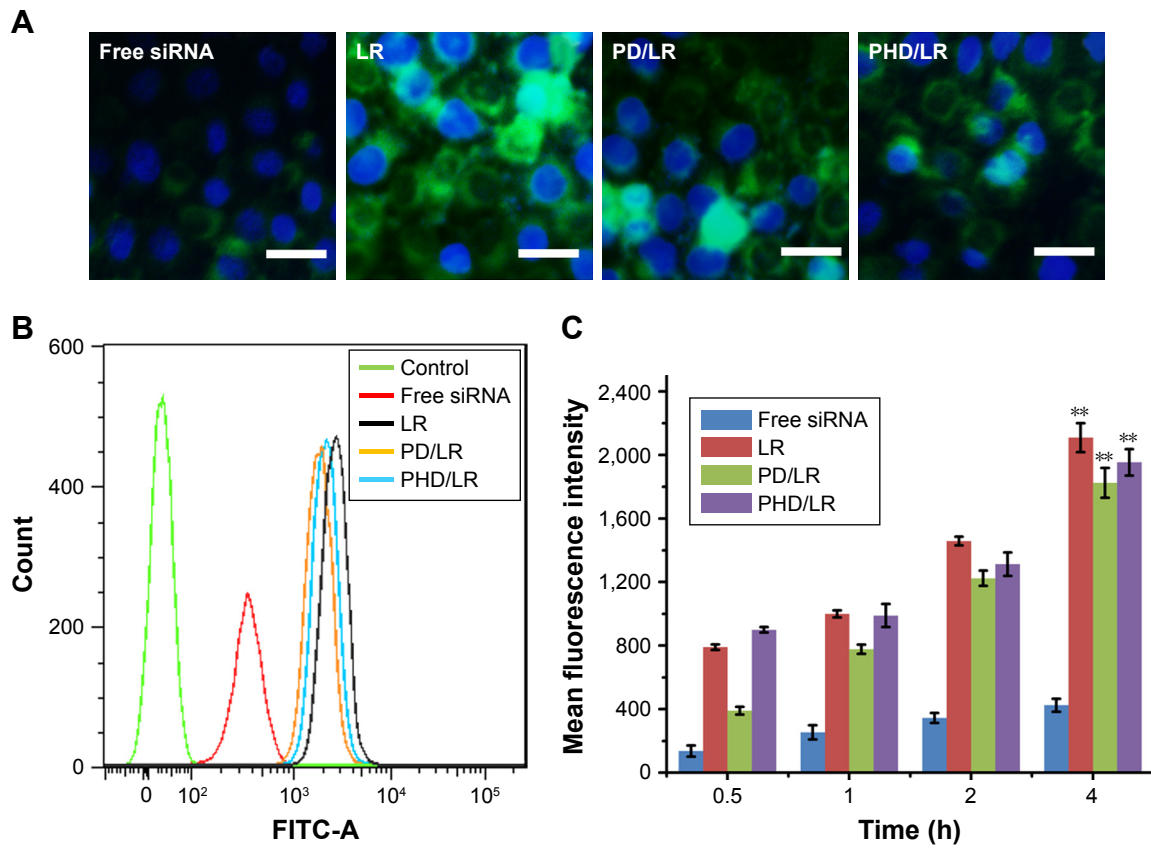


**Figure 4** Cellular uptake assay of different formulations. (A) Cellular uptake of different formulations analyzed using fluorescence microscopy. Green and blue represented siRNA and nucleic, respectively. Scale bar represented 50  $\mu$ m; flow cytometry measurement of cellular uptake of different formulations at 4 hours (B) and time-dependent cellular uptake (C).

Note: \*\* $P < 0.01$ .

Abbreviations: LR, lipoplex; mPEG, methoxy poly(ethylene glycol); PD, PHis-PSD; PHD, mPEG-PHis-PSD; PHis, poly(histidine); PSD, poly(sulfadimethoxine).

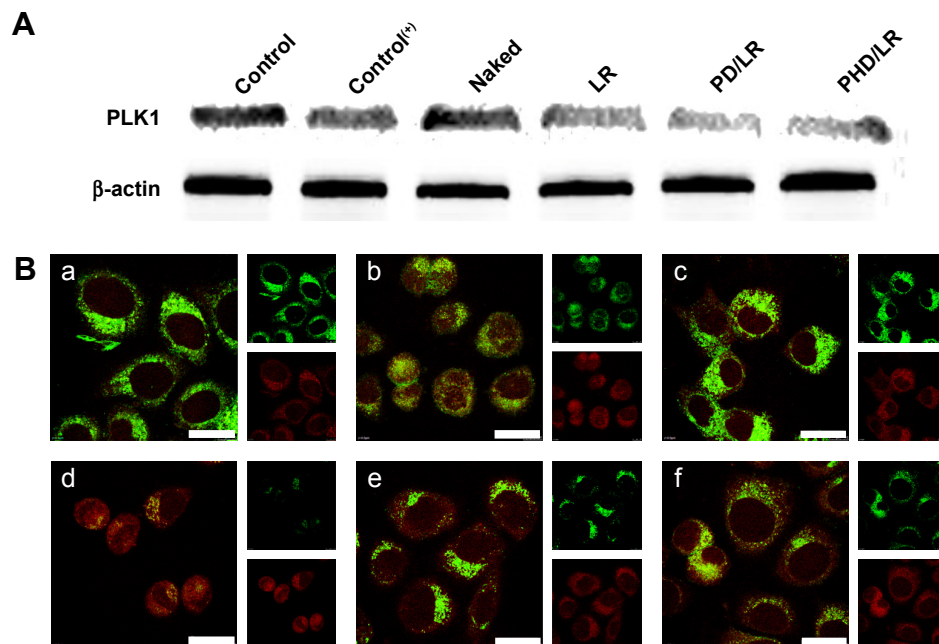


**Figure 5** In vitro PLK1 expression with Western immunoblotting (A) and immunofluorescence (B), respectively. Red and green fluorescence represents  $\beta$ -actin and PLK1, respectively. Scale bar =20  $\mu$ m (a, b, c, d, e, and f represent Control, Control<sup>(Δ)</sup>, naked siRNA, LR, PD/LR and PHD/LR, respectively).

Abbreviations: LR, lipoplex; PD, PHis-PSD; PEG, poly(ethylene glycol); PHD, PEG-PHis-PSD; PHis, poly(histidine); PSD, poly(sulfadimethoxine).

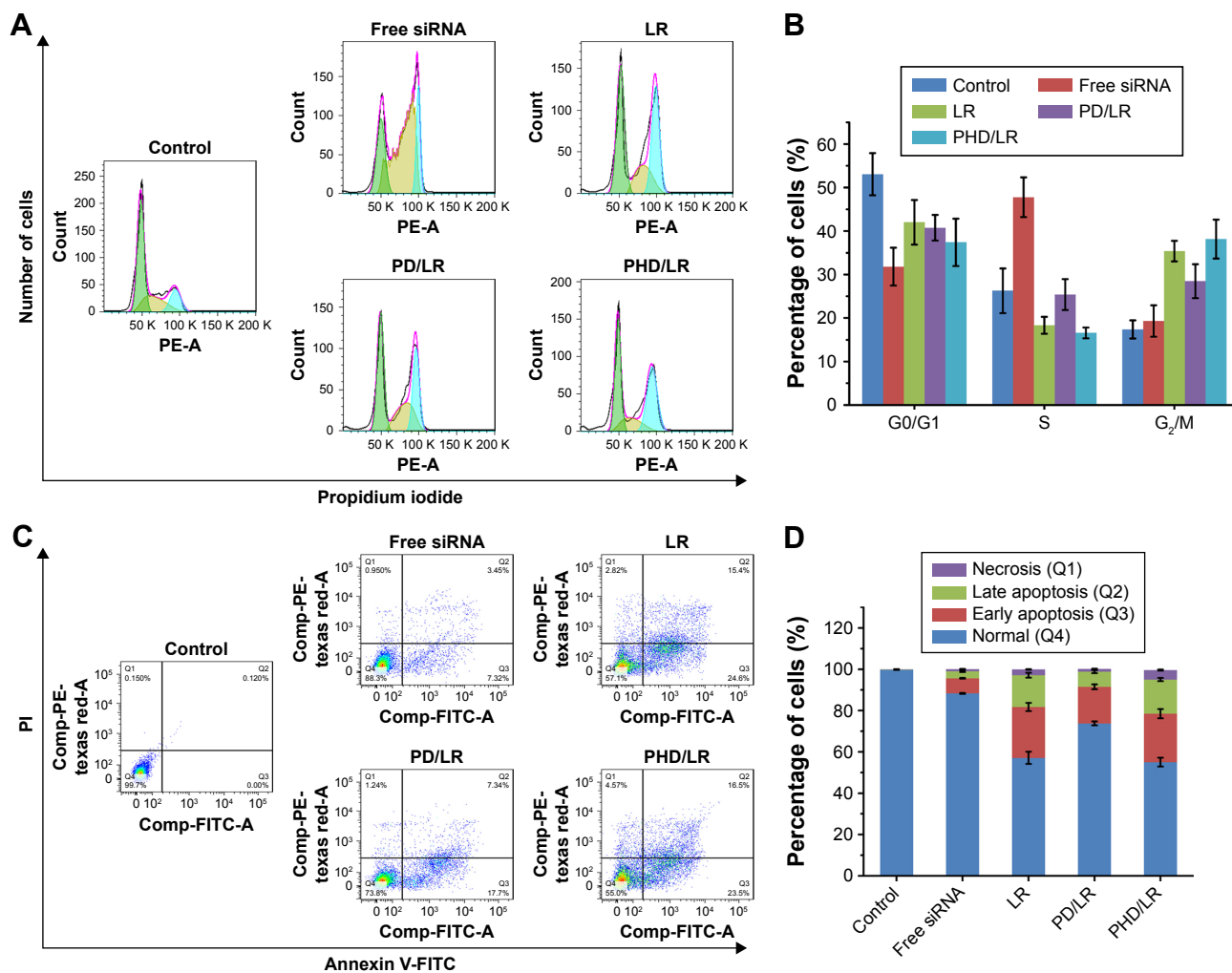


**Figure 6** Cell cycle (A and B) and apoptosis-inducing effect (C and D) of different siPLK1-formulations. **Abbreviations:** LR, lipoplex; mPEG, methoxy poly(ethylene glycol); PD, PHis-PSD; PHD, mPEG-PHis-PSD; PHis, poly(histidine); PSD, poly(sulfadimethoxine).

possessed low G<sub>2</sub>/M phase (17.37%), while siPLK1 treated groups exhibited an increase of G<sub>2</sub>/M phase percentage. G<sub>2</sub>/M phase percentage of PHD/LR group was 38.15%, indicating PHD/LR could efficiently inhibit cell cycle at G<sub>2</sub>/M phase and prevent mitosis progression. Apoptosis-inducing effect of different formulations was also investigated. As shown in Figure 6C and D, compared with control group, an increase of apoptosis cell percentage could be observed when the cells were treated with different siPLK1 formulations. PHD/LR possessed favorable apoptosis-inducing effect, and the total apoptosis cell percentage (includes early apoptosis, late apoptosis, and necrosis cells) was 45.2%, and similar result could be observed previously.

From both results, we have the reason to believe PHD/LR possessed favorable cell cycle prevention effect and apoptosis-inducing effect, and this result was of great importance for further in vivo studies.

### Endo/lysosomal escape assay

The results revealed that PHD/LR could efficiently release siRNA in acidic pH and possessed favorable antitumor activity. However, mechanism involved in the intracellular delivery of siRNA by PHD/LR was not investigated. Therefore, we observed the intracellular drug release process using LSCM. As shown in Figure 7, red, green, and blue fluorescence indicated endo/lysosomes, siRNA, and nucleic acid, respectively. Chloroquine, a weak base, was used to regulate the pH value of acidic organelles.<sup>16</sup> The presence of yellow pixel dots corresponding to the co-localization of siRNA and endo/lysosomes indicated that siRNA was in endo/lysosomes. Chloroquine-treated cells exhibited significant co-localization phenomenon at all time points, indicating that siRNA was not released into the cytoplasm. However, only few yellow pixel dots could be observed at 0.5 hours, while strong green fluorescence could be observed at the



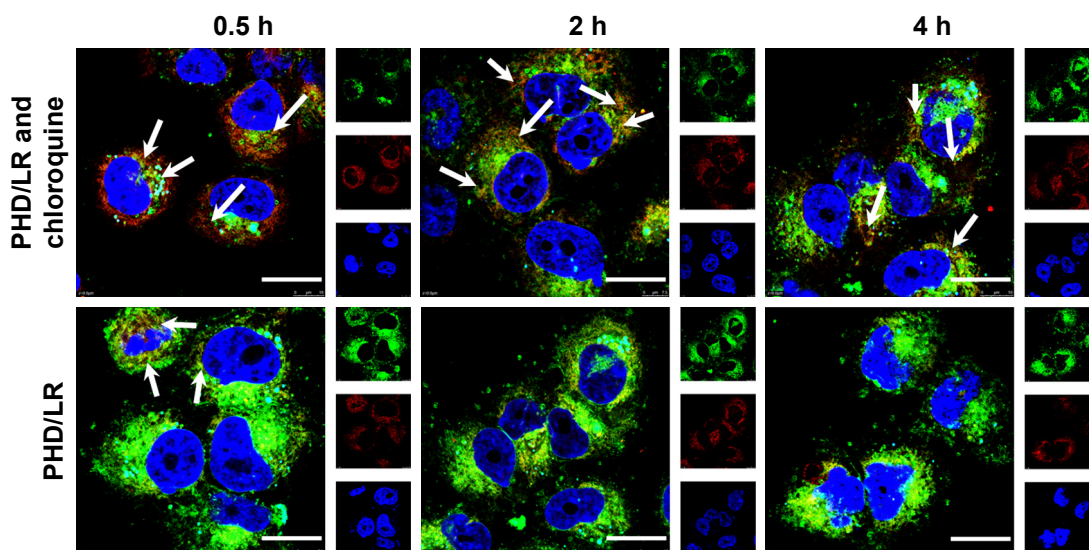


**Figure 7** LSCM observation of PHD/LR intracellular release with or without the incubation of chloroquine at different time points.

**Notes:** Green, red, and blue fluorescence indicates siRNA, endo/lysosomes, and nucleic acid, respectively. Scale bar =20  $\mu$ m.

**Abbreviations:** LR, lipoplex; LSCM, laser scan confocal microscopy; mPEG, methoxy poly(ethylene glycol); PHD, mPEG-PHis-PSD; PHis, poly(histidine); PSD, poly(sulfadimethoxine).

following time point, indicating that most of the siRNA molecules were released from endosomes into cytoplasm, which was very important for siRNA to exert its antitumor activity. Efficient endo/lysosomal escape phenomenon was mainly attributed to acidic pH, where PSD would reverse the charge from negative to neutral and dissociate from LR, and PHis segment in acidic pH would protonate and show proton sponge effect to increase the permeability of endosome membrane. The synergistic effects of these segments facilitated increased siRNA concentration in cytoplasm and increased therapeutical efficacy. Although the existence of PEG shell would decrease cellular uptake, efficient endo/lysosome escape would make up this disadvantage and increase the therapeutical effect.

### In vivo biodistribution assay

The results indicated that LR possessed favorable siRNA delivery efficacy while PEG introduction seemed to be unnecessary. In fact, there are many barriers when the formulations are administered intravenously into the blood system. The presence of PEG would significantly avoid the elimination of RES and enhance in vivo circulation time. To validate this viewpoint, in vivo biodistribution assay was carried out. As shown in Figure S3A and B, DiR group showed a whole body biodistribution with moderate fluorescence intensity, which indicated that free DiR was easy to be eliminated and did not exhibit specific biodistribution capability. In comparison, the fluorescence was relatively strong in tumor region for LR group, indicating LR would accumulate into tumor tissue

via EPR effect. Hopefully, PD/LR and PHD/LR possessed the best tumor accumulation capability compared with LR. This phenomenon was mainly because the introduction of PEG would avoid the elimination and enable the accumulation of high concentrations of DiR in the tumor site. The sections of major organs also indicated that PEGylated formulations could decrease the accumulation in liver and increase tumor accumulation. All these results demonstrated PHD/LR possessed favorable tumor targetability in vivo.

### In vivo antitumor activity

From all the in vitro results, we could observe that LR possessed favorable antitumor activity, which was better than PHD/LR and PD/LR. It seemed that the decoration of copolymer on the surface of LR was unnecessary. In fact, it is very important for DDS to be modified with PEG or other copolymer in order to enhance circulation time and in vivo stability. To validate this viewpoint, in vivo antitumor activity was carried out. As shown in Figure 8A, C, and D, compared with control group, free siRNA group showed a moderate antitumor effect, which was mainly because naked siRNA was easy to be degraded in complex blood environment. LR showed a slightly higher antitumor activity compared with siRNA group, indicating LR could deliver siRNA to tumor sites via EPR effect. However, this result was far from satisfactory. PD/LR possessed significantly higher antitumor activity compared with LR; this phenomenon was mainly attributed to the existence of PEG which helped in the enhancement of circulation time and

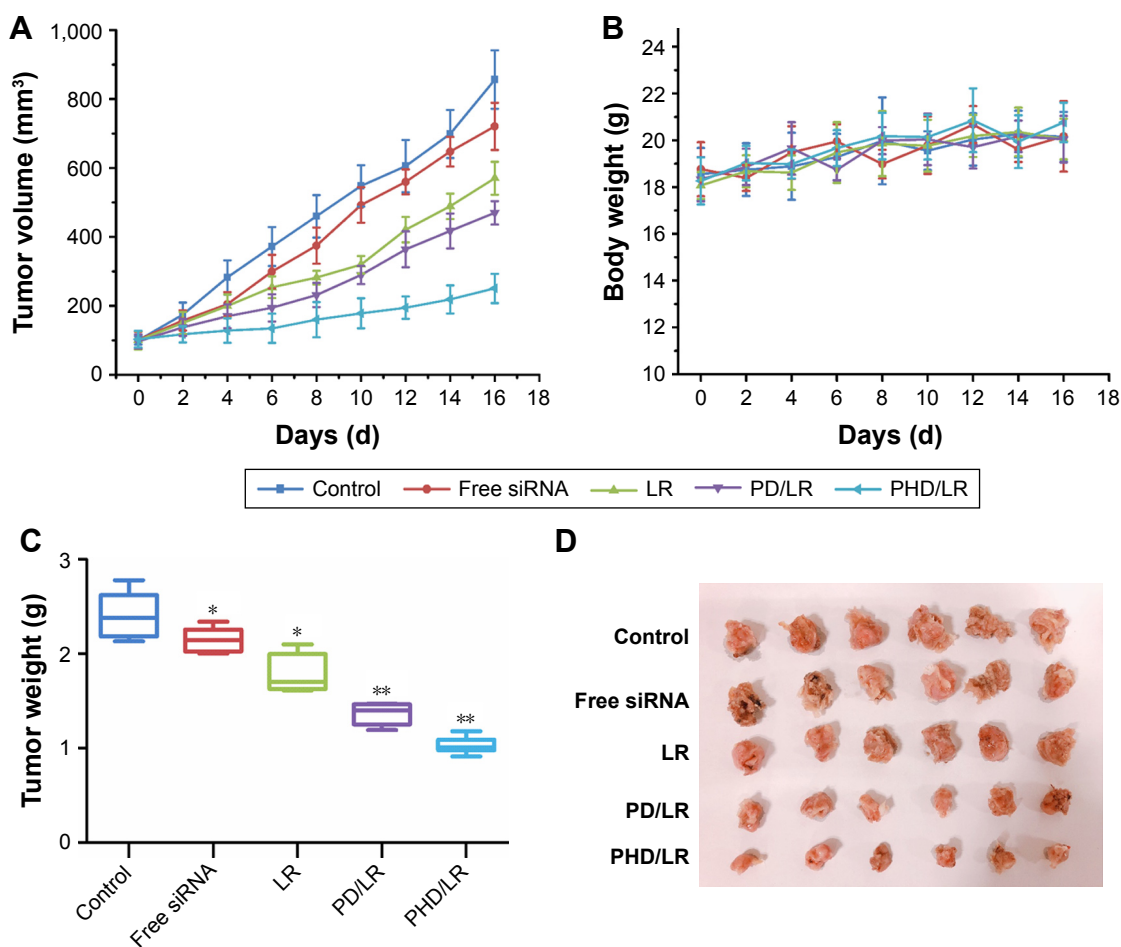


**Figure 8** In vivo antitumor activity of different drug-loaded formulations. Tumor volume (A), body weight (B), tumor weight (C), and the images of tumor (D) of different groups were recorded.

**Notes:** \* $P < 0.05$ , \*\* $P < 0.01$ .

**Abbreviations:** LR, lipoplex; mPEG, methoxy poly(ethylene glycol); PD, PHis-PSD; PHD, mPEG-PHis-PSD; PHis, poly(histidine); PI, propidium iodide; PSD, poly(sulfadimethoxine).

instantaneous dissociation in tumor acidic endo/lysosomes to release siRNA. PHD/LR possessed the best antitumor activity among all the reference groups, which can be attributed to the synergistic effect of enhanced circulation time, instantaneous dissociation, and proton sponge effect. Body weight of different groups were also measured (Figure 8B). Compared with control group, no significant decrease in body weight was observed for all groups, indicating this DDS is safe for intravenous administration.

## Histological assay

Tumor tissues were obtained to prepare paraffin-embedded tissue slides or extracted protein from tumor tissue for further use. As shown in Figure 9A–C, ex vivo PLK1 expression was also investigated using WB and IF, respectively. PHD/LR possessed the best PLK1 in vivo knockdown capability among all the reference groups, and this result was consistent with in vivo antitumor activity assay. H&E staining images

(Figure 9D) indicated that PHD/LR could efficiently kill tumor cells (the presence of voids indicated dead cells) and exhibit antitumor activity. TUNEL assay further validated that PHD/LR could induce apoptosis effect in tumor tissue and aid in cancer therapy.

## Conclusion

In this paper, a novel triblock copolymer (PHD) was first synthesized and used to construct multifunctional DDS with pH-induced charge-reversal property and proton sponge effect for efficiently delivering therapeutic gene siPLK1 into cytoplasm for lung cancer treatment. This novel DDS could efficiently load siRNA with high EE (%) and excellent stability. The resulting hybrid nanoparticle possessed high capability to deliver siRNA into cytoplasm and efficiently knockdown PLK1 expression. All the in vitro and in vivo studies indicated that PHD/LR was a suitable gene carrier for cancer therapy.

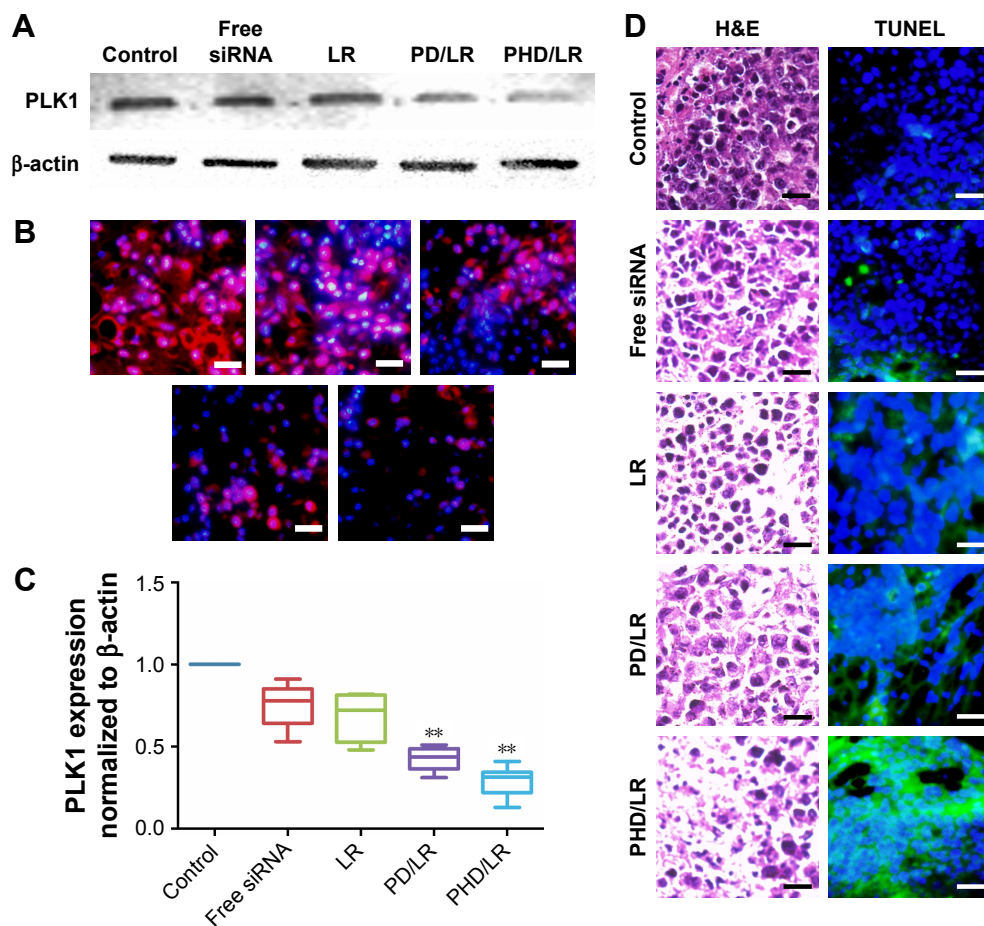


**Figure 9** Ex vivo PLK1 expression detected using WB (A) and IF (B), respectively. PLK1 expression was also quantified (C). Tumor tissues were used to prepare paraffin-embedded slides for H&E and TUNEL study (D).

**Notes:** \*\* $P < 0.01$ , scale bars represent 50  $\mu$ m.

**Abbreviations:** IF, immunofluorescence; LR, lipoplex; mPEG, methoxy poly(ethylene glycol); PD, PHis-PSD; PHD, mPEG-PHis-PSD; PHis, poly(histidine); PSD, poly(sulfadimethoxine); WB, Western blotting.

## Acknowledgment

The authors are grateful for the financial support of the National Natural Science Foundation of China (81202483, 81773668, and 81302721).

## Disclosure

The authors report no conflicts of interest in this work.

## References

- Remon J, Vilarino N, Reguart N. Immune checkpoint inhibitors in non-small cell lung cancer (NSCLC): Approaches on special subgroups and unresolved burning questions. *Cancer Treat Rev*. 2018;64:21–29.
- Li T, Ding ZL, Zheng YL, Wang W. MiR-484 promotes non-small-cell lung cancer (NSCLC) progression through inhibiting Apaf-1 associated with the suppression of apoptosis. *Biomed Pharmacother*. 2017; 96:153–164.
- Leonetti A, Facchinetti F, Rossi G, et al. BRAF in non-small cell lung cancer (NSCLC): Pickaxing another brick in the wall. *Cancer Treat Rev*. 2018;66:82–94.
- Osuoha CA, Callahan KE, Ponce CP, Pinheiro PS. Disparities in lung cancer survival and receipt of surgical treatment. *Lung Cancer*. 2018; 122:54–59.
- Brustugun OT, Grønberg BH, Fjellbirkeland L, et al. Substantial nation-wide improvement in lung cancer relative survival in Norway from 2000 to 2016. *Lung Cancer*. 2018;122:138–145.
- Zhang J, Du Z, Pan S, et al. Overcoming Multidrug Resistance by Code-livery of MDR1-Targeting siRNA and Doxorubicin Using EphA10-Mediated pH-Sensitive Lipoplexes: In Vitro and In Vivo Evaluation. *ACS Appl Mater Interfaces*. 2018;10(25):21590–21600.
- Zhang J, Chen K, Ding Y, et al. Self-assembly of pH-responsive dextran-g-poly(lactide-co-glycolide)-g-histidine copolymer micelles for intracellular delivery of paclitaxel and its antitumor activity. *RSC Adv*. 2016;6(28):23693–23701.
- Zhang J, Luo Y, Zhao X, et al. Co-delivery of doxorubicin and the traditional Chinese medicine quercetin using biotin-PEG 2000-DSPE modified liposomes for the treatment of multidrug resistant breast cancer. *RSC Adv*. 2016;6(114):113173–113184.
- Zang X, Ding H, Zhao X, et al. Anti-EphA10 antibody-conjugated pH-sensitive liposomes for specific intracellular delivery of siRNA. *Int J Nanomedicine*. 2016;11:3951–3967.
- Zhu J, Qiao M, Wang Q, et al. Dual-responsive polyplexes with enhanced disassembly and endosomal escape for efficient delivery of siRNA. *Biomaterials*. 2018;162:47–59.
- Wang HX, Yang XZ, Sun CY, Mao CQ, Zhu YH, Wang J. Matrix metalloproteinase 2-responsive micelle for siRNA delivery. *Biomaterials*. 2014;35(26):7622–7634.

12. Tang S, Meng Q, Sun H, et al. Dual pH-sensitive micelles with charge-switch for controlling cellular uptake and drug release to treat metastatic breast cancer. *Biomaterials*. 2017;114:44–53.
13. Yan T, Cheng J, Liu Z, Cheng F, Wei X, He J. pH-Sensitive mesoporous silica nanoparticles for chemo-photodynamic combination therapy. *Colloids Surf B Biointerfaces*. 2018;161:442–448.
14. Luo M, Jia YY, Jing ZW, et al. Construction and optimization of pH-sensitive nanoparticle delivery system containing PLGA and UCCs-2 for targeted treatment of *Helicobacter pylori*. *Colloids Surf B Biointerfaces*. 2018;164:11–19.
15. Li XX, Chen J, Shen JM, et al. pH-Sensitive nanoparticles as smart carriers for selective intracellular drug delivery to tumor. *Int J Pharm*. 2018;545(1–2):274–285.
16. Zhang J, Zhao X, Chen Q, et al. Systematic evaluation of multi-functional paclitaxel-loaded polymeric mixed micelles as a potential anticancer remedy to overcome multidrug resistance. *Acta Biomater*. 2017;50:381–395.
17. Zhang J, Yang C, Pan S, et al. Eph A10-modified pH-sensitive liposomes loaded with novel triphenylphosphine-docetaxel conjugate possess hierarchical targetability and sufficient antitumor effect both in vitro and in vivo. *Drug Deliv*. 2018;25(1):723–737.
18. Chen Q, Ding H, Zhou J, et al. Novel glycyrrhetic acid conjugated pH-sensitive liposomes for the delivery of doxorubicin and its antitumor activities. *RSC Adv*. 2016;6(22):17782–17791.
19. Masson C, Garinot M, Mignet N, et al. pH-sensitive PEG lipids containing orthoester linkers: new potential tools for nonviral gene delivery. *J Control Release*. 2004;99(3):423–434.
20. Wang A, Gui L, Lu S, Zhou L, Zhou J, Wei S. Tumor microenvironment-responsive charge reversal zinc phthalocyanines based on amino acids for photodynamic therapy. *Dyes and Pigments*. 2016;126:239–250.
21. Naem M, Oshi MA, Kim J, et al. pH-triggered surface charge-reversal nanoparticles alleviate experimental murine colitis via selective accumulation in inflamed colon regions. *Nanomed Nanotechnol Biol Med*. 2018;14(3):823–834.
22. Gou J, Liang Y, Miao L, et al. Improved tumor tissue penetration and tumor cell uptake achieved by delayed charge reversal nanoparticles. *Acta Biomater*. 2017;62:157–166.
23. Hu J, Miura S, Na K, Bae YH. pH-responsive and charge shielded cationic micelle of poly(L-histidine)-block-short branched PEI for acidic cancer treatment. *J Control Release*. 2013;172(1):69–76.
24. Han SK, Na K, Bae YH. Sulfonamide based pH-sensitive polymeric micelles: physicochemical characteristics and pH-dependent aggregation. *Colloids Surf A Physicochem Eng Asp*. 2003;214(1–3):49–59.
25. Zhou Z, Badkas A, Stevenson M, Lee JY, Leung YK. Herceptin conjugated PLGA-PHis-PEG pH sensitive nanoparticles for targeted and controlled drug delivery. *Int J Pharm*. 2015;487(1–2):81–90.
26. Zhang X, Chen D, Ba S, et al. Poly(L-histidine) based copolymers: Effect of the chemically substituted L-histidine on the physio-chemical properties of the micelles and in vivo biodistribution. *Colloids Surf B Biointerfaces*. 2016;140:176–184.
27. Hong W, Chen D, Jia L, et al. Thermo- and pH-responsive copolymers based on PLGA-PEG-PLGA and poly(L-histidine): synthesis and in vitro characterization of copolymer micelles. *Acta Biomater*. 2014;10(3):1259–1271.
28. Zhao XY, Nie CL, Liang SF, Yuan Z, Deng HX, Wei YQ. Enhanced gemcitabine-mediated cell killing of human lung adenocarcinoma by vector-based RNA interference against PLK1. *Biomed Pharmacother*. 2012;66(8):597–602.
29. Liu Z, Sun Q, Wang X. PLK1, A Potential Target for Cancer Therapy. *Transl Oncol*. 2017;10(1):22–32.
30. Shen J, Song G, An M, et al. The use of hollow mesoporous silica nanospheres to encapsulate bortezomib and improve efficacy for non-small cell lung cancer therapy. *Biomaterials*. 2014;35(1):316–326.
31. Liang H, Ren X, Qian J, et al. Size-Shifting Micelle Nanoclusters Based on a Cross-Linked and pH-Sensitive Framework for Enhanced Tumor Targeting and Deep Penetration Features. *ACS Appl Mater Interfaces*. 2016;8(16):10136–10146.
32. Singla AK, Garg A, Aggarwal D. Paclitaxel and its formulations. *Int J Pharm*. 2002;235(1–2):179–192.
33. Gumireddy K, Reddy MV, Cosenza SC, et al. ON01910, a non-ATP-competitive small molecule inhibitor of Plk1, is a potent anticancer agent. *Cancer Cell*. 2005;7(3):275–286.



## Supplementary materials

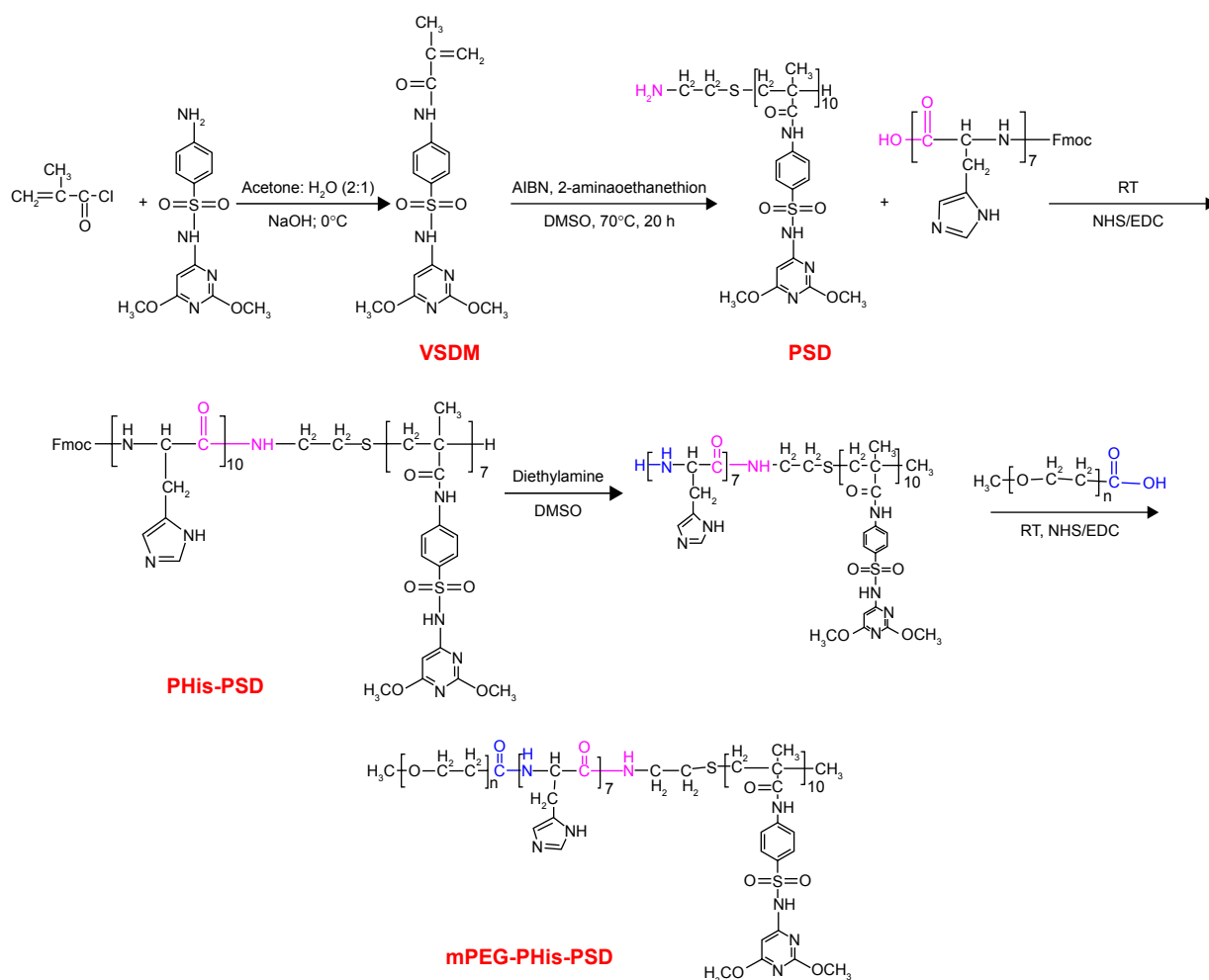


**Figure S1** Synthesis pathway of PHD copolymer.

**Abbreviations:** mPEG, methoxy poly(ethylene glycol); PHD, mPEG-PHis-PSD; PHis, poly(histidine); PSD, poly(sulfadimethoxine); VSDM, vinylated SD.

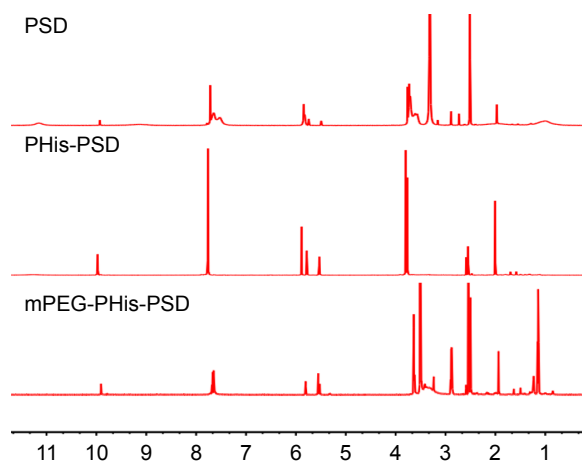


**Figure S2** Typical <sup>1</sup>H-NMR spectrum of different copolymers.

**Abbreviations:** mPEG, methoxy poly(ethylene glycol); PHis, poly(histidine); PSD, poly(sulfadimethoxine).

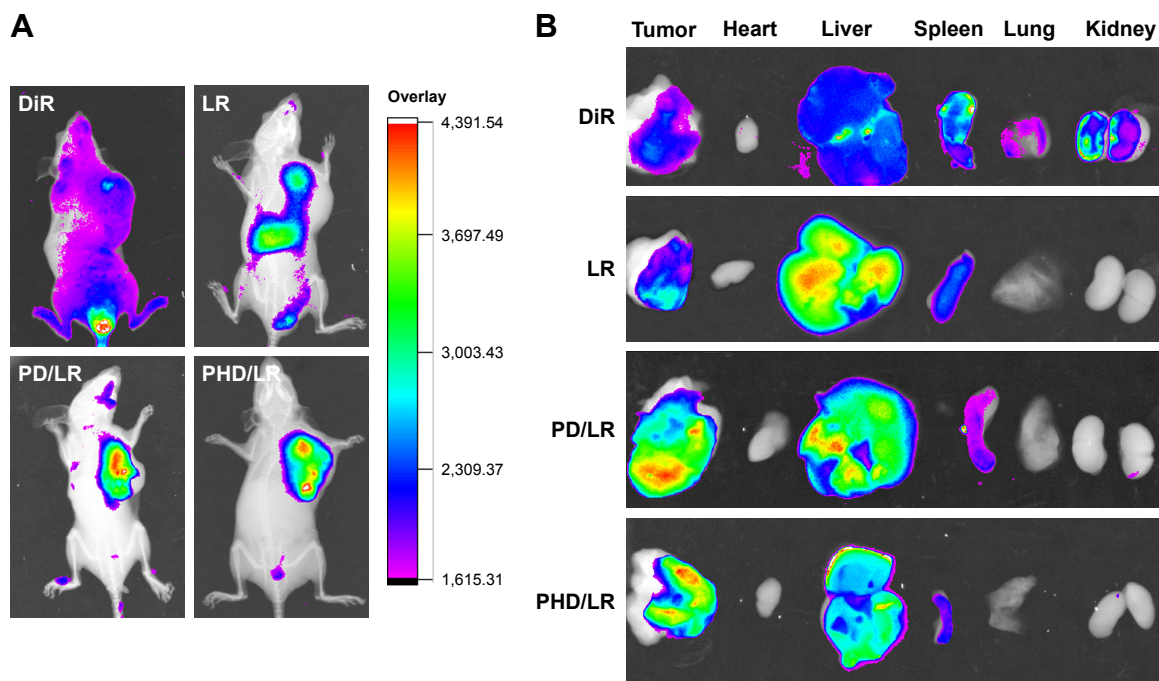


**Figure S3** In vivo biodistribution assay of nude mice. **(A)** in vivo biodistribution assay of nude mice bearing A549 tumor. **(B)** After 24 h, mice were sacrificed the the major organs were obtained for detecting biodistribution of different formulations in different organs.

**Notes:** The mice were intravenously injected with different DiR-loaded formulations with the same DiR concentration. Major organs were obtained and observed at the end of the study.

**Abbreviations:** DiR, 1, 10-dioctadecyl-3, 3, 30, 30-tetramethyl indotricarbocyanine iodide; LR, lipoplex; mPEG, methoxy poly(ethylene glycol); PD, PHis-PSD; PHD, mPEG-PHis-PSD; PHis, poly(histidine); PSD, poly(sulfadimethoxine).